Theoretical and Experimental Investigation on the Oxidation of Gallic Acid by Sulfate Radical Anions

Paula Caregnato,[†] Pedro M. David Gara,[†] Gabriela N. Bosio,[†] Mónica C. Gonzalez,[†] Nino Russo,*,[‡] María del Carmen Michelini,[‡] and Daniel O. Mártire*,[†]

Instituto de Investigaciones Fisicoquímicas Teóricas y Aplicadas (INIFTA), Facultad de Ciencias Exactas, Universidad Nacional de La Plata, C. C. 16, Suc. 4, (1900) La Plata, Argentina and Dipartimento di Chimica, Università della Calabria, Via P. Bucci, Cubo 14 C, 87030 Arcavacata di Rende, Italy

By monitoring the decay of $SO_4^{\bullet-}$ after flash photolysis of aqueous solutions of $S_2O_8^{2-}$ at different pH values, the kinetics of the reaction of $SO_4^{\bullet-}$ radicals with gallic acid and the gallate ion was investigated. The bimolecular rate constants for the reactions of the sulfate radicals with gallic acid and the gallate ion were found to be $(6.3 \pm 0.7) \times 10^8$ and $(2.9 \pm 0.2) \times 10^9$ M^{-1} s^{-1}, respectively. On the basis of the oxygen-independent second-order decay kinetics and on their absorption spectra, the organic radicals formed as intermediates of these reactions were assigned to the corresponding phenoxyl radicals. DFT calculations in the gas phase and aqueous solution support formation of the phenoxyl radicals by H abstraction from the phenols to the sulfate radical anion. The observed recombination of the phenoxyl radicals of gallic acid to yield substituted biphenyls and quinones is also supported by the calculations. HPLC/MS product analysis showed formation of one of the predicted quinones.

Introduction

Humic substances (HS) widely distribute in aqueous and soil environments. HS are weak-acid polyelectrolytes with a variety of abilities, such as reducing to Cr(VI),[1] complexing of heavy-metal ions,[2] and solubilization of hydrophobic chemicals,[3] which may cause concern with the fate of pollutants in the environment.

Photoreduction of Fe(III) to Fe(II) was reported to be accelerated in the presence of HS, which contain a variety of carboxylic groups, such as phenolic acids and fatty acids.[4] Phenolic hydroxyl groups concern the reducing abilities of HS,[1] while the carboxylic moieties are relevant for complexation of metal ions, such as iron.[5] HS are involved in important chemical, biochemical, and photochemical processes occurring in soil and water systems.[6−10] The equilibria between structural polyphenolic and quinonoid units result in semiquinonoid radicals.[11,12]

In situ chemical oxidation (ISCO) is a method based on the injection of chemical oxidants into the source zone in order to destroy the contaminants by converting them to substances such as carbon dioxide, water, and inorganic acids.[13−18] Destruction of organic compounds by free-radical-based activated peroxodisulfate oxidation in contaminated waters and soils is gaining interest as an ISCO technology.[13−16] Peroxodisulfate oxidation is generally carried out under heat-, photo-, acid-, base-, or metal-activated conditions because oxidation rates can be greatly accelerated by formation of sulfate radicals ($SO_4^{\bullet-}$).[17−18] Under these conditions, HS will compete with the contaminants for the produced $SO_4^{\bullet-}$ radicals. For this reason we are interested in the mechanistic aspects of the interaction of the sulfate radicals with HS.

Given the complex nature of HS, an approach toward a better understanding of their structure and interactions is to use low molecular weight model compounds with well-known physicochemical properties. The choice of these model molecules stemmed largely from the evidence that HS consist mainly of carboxy and phenolic moieties.[19,20] Giannakopoulos et al. investigated the influence of Pb(II) on the radical properties of humic substances and found that gallic and tannic acids are good working models for the radical properties of humic acid and fulvic acid.[21]

In a first approximation we started with the mechanistic investigation of the reaction of the sulfate radicals with gallic acid. On the other hand, formation of oxidized radicals of gallic acid is also of biological interest.[22]

Here we generated sulfate radicals by flash photolysis of $S_2O_8^{2-}$, reaction 1.[23]

$$S_2O_8^{2-} + h\nu \rightarrow 2SO_4^{\bullet-} \qquad (1)$$

Gallic acid, the 3,4,5-trihydroxybenzoic acid, has pK_a values of 4.4, 8.2, 10.7, and 13.1.[24] By monitoring the decay of $SO_4^{\bullet-}$ after flash photolysis of aqueous solutions of $S_2O_8^{2-}$ in the presence of gallic acid in solutions at pH 3.1 and 5.4, we investigated the kinetics of the reaction of $SO_4^{\bullet-}$ radicals with gallic acid and the gallate ion, respectively, and the decay and absorption spectra of the organic radicals generated.

Experimental Methods

Materials. Gallic acid, $Na_2S_2O_8$, NaOH, KOH, and $HClO_4$ (all from Merck) and $NaBH_4$ (Riedel-de Haën), glycine (Sigma-Aldrich), and Nitro Blue Tetrazolium (NBT; GIBCO S.R.L.) were used without further purification. Distilled water (>18 MΩ

* To whom correspondence should be addressed. (N.R.) Phone: -390984/ 492106. Fax: -39 0984 493 390. E-mail: nrusso@unical.it. (D.O.M.) Phone: -54 221 4257430/7291. Fax: -54 221 4254642. E-mail: dmartire@ inifta.unlp.edu.ar.
† Universidad Nacional de La Plata.
‡ Università della Calabria.

Oxidation of Gallic Acid by Sulfate Radical Anions

J. Phys. Chem. A, Vol. 112, No. 6, 2008 **1189**

cm^{-1}, <20 ppb of organic carbon) was obtained from a Millipore system.

Laser Flash Photolysis (LFP) Experiments. LFP experiments were performed by excitation with the fourth harmonic of a Nd:YAG Litron laser (2 ns fwhm and 6 mJ per pulse at 266 nm). The analysis light from a 150 W Xe arc lamp was passed through a monochromator (PTI 1695) and detected by a 1P28 PTM photomultiplier. A 10 mm path length cuvette was employed. Decays typically represented the average of 64 pulses and were taken by and stored in a 500 MHz Agilent Infiniium oscilloscope. The solutions had an absorbance of 0.5 at 266 nm, and less than 6% of the incident light was absorbed by gallic acid or gallate ion, which guarantees that photolysis of these substrates is negligible under our experimental conditions.

Conventional Flash Photolysis (CFP) Experiments. CFP experiments were done with a Xenon Co. model 720C equipment with modified optics and electronics.[23] The optical path length of the reaction cell is 100 mm. The analysis source was a high-pressure mercury lamp (Osram XBO 75W/2 and Ushio XE 75W). The emission of the flash lamps was filtered with an aqueous solution highly concentrated in gallic acid/gallate ion in order to prevent photolysis of the substrate. To avoid product accumulation, each solution was irradiated only once. Signals arising from single shots were averaged.

Product Analysis. To analyze the reaction products, 0.01 M $S_2O_8^{2-}$ solutions containing 10^{-5} M gallic acid at pH 3.1 and 5.4 were irradiated with five flashes of the CFP pulsed lamps to increment the product concentration. The quinones test was performed in both solutions, and only that of pH 5.4 was analyzed by HPLC/MS.

Quinones Test. The NBT/glycinate assay[25] was used to detect production of quinones. A 100 μL amount of the irradiated solution was mixed at 4 °C with 300 μL of 2 M potassium glycinate (pH = 10), 100 μL of 10 mg/mL sodium borohydride, and 1 mL of 0.24 mM NBT solution prepared in 2 M potassium glycinate at pH = 10. The reaction was started by incubating the mixture in a water bath at 25 °C in the dark. After 1 h, the absorbance at 530 nm was measured using a CARY13 spectrophotometer.

HPLC/MS. The samples were analyzed with an Agilent 1100 LC-MS modular system. The configuration was as follows: binary pump, diode array detector, and mass-selective detector using API-ES interface (electrospray). A Restek Pinnacle II C18 5 μm column was used. The solvent was a 1:1 methanol:water mixture. The flow rate was 1 mL/min, and the injection volume was 20 μL. The MSD parameters were as follows: API-ES positive mode and mass range 60−400 amu.

Theoretical Methodology. Density functional theory (DFT) in its three-parameter hybrid B3LYP[26,27] formulation together with the 6-311++G** extended basis set[28−30] was the computational methodology used in the present work. All calculations were carried out with the GAUSSIAN03 code.[31]

All geometrical structures reported here were fully optimized. Vibrational frequency calculations were carried out to confirm the local minima character of the species and determine the zero-point vibrational energies and thermal corrections to the Gibbs free energies. The unrestricted open-shell approach was used for radical species. No spin contamination was found for the radicals, as the deviation of the calculated $\langle S^2 \rangle$ value was less than 5% with respect to the expected theoretical value, i.e., 0.750.

Solvent effects were computed within the framework of the self-consistent reaction field polarized continuum model (SCRF-IEF-PCM)[32−34] as implemented in the Gaussian03 package. The
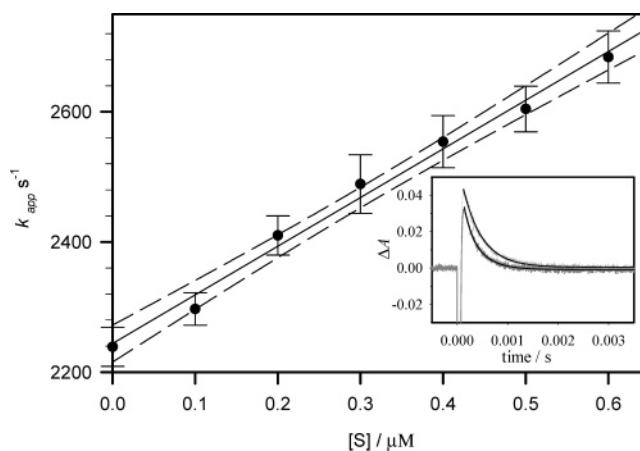

Figure 1. Plots of k_{app} vs substrate concentration obtained with 0.01 M $Na_2S_2O_8$ solutions at 293 K: at pH 3.1. The values of k_{app} for each concentration are the average rate constants obtained from at least four independent experiments. The error bars stand for the standard deviations, and the dashed lines show the 99% confidence interval. (Inset) Absorbance decay traces obtained at $\lambda = 450$ nm with solutions containing 0 (A) and 6×10^{-7} M (B) gallic acid at pH 3.1.

TABLE 1: Bimolecular Rate Constants for the Reaction of Sulfate Radical with the Gallic Species

$k_2^{Ga}/M^{-1} s^{-1}$ [a]	$k_2^{GaH}/M^{-1} s^{-1}$ [b]
$(2.9 \pm 0.2) \times 10^9$	$(6.3 \pm 0.7) \times 10^8$

[a] The error bar in k_2^{Ga} is the standard deviation obtained from the linear correlation between k_{app} and [S]. [b] The error bar in k_2^{GaH} is obtained from an error propagation analysis of eq 3 taking the values of 0.5×10^8 M^{-1} s^{-1}, 0.2×10^9 M^{-1} s^{-1}, 0.01, and 0.1 for the error bars of s, k_2^{Ga}, pH, and pK_a, respectively.

default UAO[31] set of solvation radii was used in the calculations to build the cavity according to the molecular topology, hybridization, and formal charge. In this method, the solvent was modeled as a continuum of dielectric constant ϵ. The solute was placed in a cavity within the solvent. The polarized continuum model, in particular, defines the cavity as the union of a series of interacting spheres centered on the atoms and uses a numerical representation of the polarization of the solvent. This type of model, however, does not consider specific interactions between the solute and the solvent.

Results and Discussion

Reaction of Sulfate Radicals with Gallic Acid. Reactions of $SO_4^{•-}$ radicals with solutions of gallic acid at pH (3.1 ± 0.1) and (5.4 ± 0.1), where the main species are the gallic acid and its conjugated species, respectively, are conveniently studied following the $SO_4^{•-}$ radical decay rate as a function of added substrate concentration. Photolysis experiments of $S_2O_8^{2-}$ in the presence of low concentrations of gallic acid showed absorption traces at $\lambda > 400$ nm, whose spectrum immediately after the flash of light agreed with that of the sulfate radical ions. The absorption traces taken at $\lambda = 450$ nm showed faster decay kinetics with increasing concentrations of the organic substrates (S) and could be well fitted to $\Delta A = \Delta A_0 \exp(-k_{app}t) + C$ (Figure 1, inset). The very small constant term C (lower than 1% the maximum absorbance) is associated with the absorption of a longer lived species, i.e., the organic radicals formed by reaction 2. The slope of the linear plots of k_{app} vs substrate concentration obtained from experiments at pH = 5.4 yields
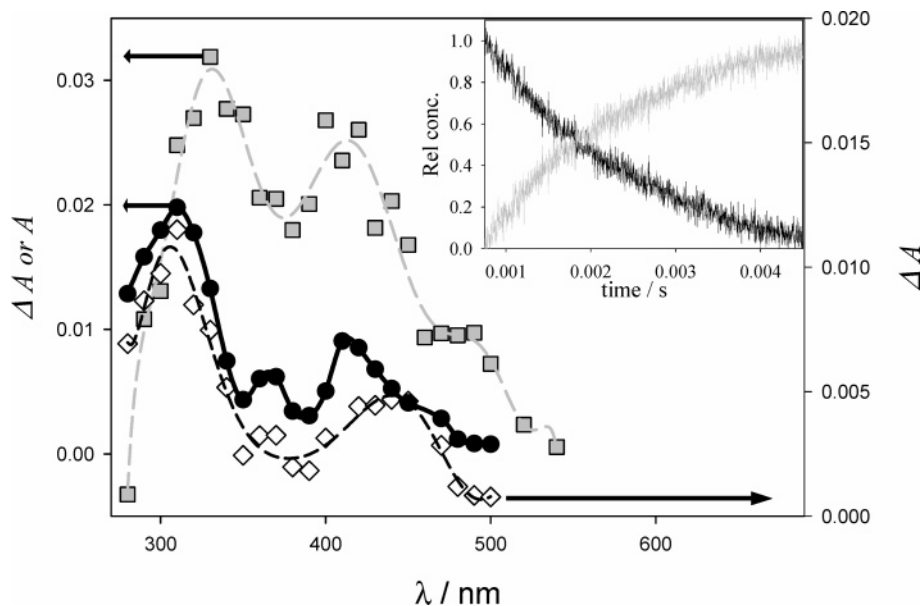
Figure 2. Absorption spectra obtained in LFP experiments with 5×10^{-2} M Na₂S₂O₈ containing 50 μM gallic at pH 3.1 taken 5 (●) and 50 μs (◇) after the laser shot. Absorption spectrum of the products (gray squares) obtained in CFP experiments with 1×10^{-2} M Na₂S₂O₈ containing 5 μM gallic at pH 3.1 obtained from the bilinear program. (Inset) Decay of the shorter lived (in black) and formation of the longer lived (in gray) species obtained from the bilinear analysis of the CFP experiments of the main figure.
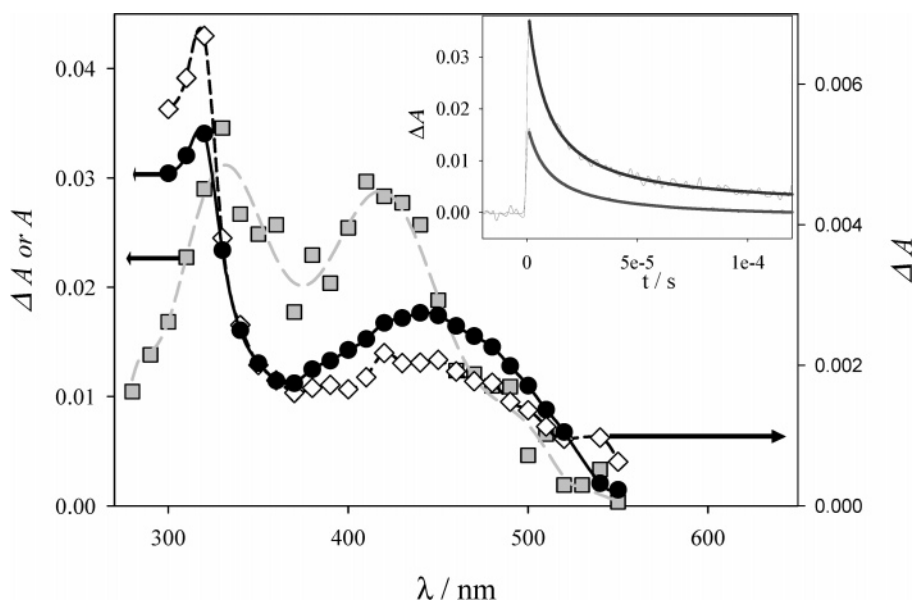
Figure 3. Absorption spectra obtained in LFP experiments with 5×10^{-2} M Na₂S₂O₈ containing 50 μM gallic at pH 5.4 taken 2 (●) and 50 μs (◇) after the laser shot. Absorption spectrum of the products (gray squares) obtained in CFP experiments with 1×10^{-2} M Na₂S₂O₈ containing 5 μM gallic at pH 5.4 obtained from the bilinear program. (Inset) LFP experimental traces obtained at $\lambda = 320$ (upper trace) and 400 nm (lower trace).

the bimolecular rate constants k_2^{Ga} (for S = gallate ion), shown in Table 1.

$$SO_4^{\bullet-} + S \rightarrow \text{organic radicals} \qquad (2)$$
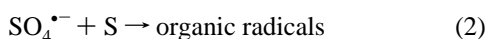
The absolute rate constant k_2 for gallic acid, k_2^{GaH}, listed in Table 1 is obtained from eq 3

$$k_2^{GaH} = (s - k_2^{Ga}) \times 10^{(pH - pK_a)} + s \qquad (3)$$

where $s = (7.4 \pm 0.5) \times 10^8$ M⁻¹ s⁻¹ is the slope of the straight line shown in Figure 1, $k_2^{Ga} = (2.9 \pm 0.2) \times 10^9$ M⁻¹ s⁻¹, and $pK_a = 4.4$ (see above).

Detection of the Organic Radicals. To obtain further information on reaction 2, the nature of the organic radicals was investigated. To that purpose, peroxodisulfate solutions containing gallic acid (both at pH 3.1 and 5.4) at concentrations of 50 and 5 μM were employed for the LFP and CFP experiments, respectively.

LFP experiments in the absence of added gallic acid show formation of sulfate radicals, which decay with mixed first- and second-order kinetics. From the traces obtained at 450 nm taking 1650 M⁻¹ cm⁻¹ for the absorption coefficient of the sulfate radicals at this wavelength,[35] the initial sulfate radical concentration of 5.3×10^{-6} M is obtained. The decay observed in the experiments without added gallic acid and the rate expected

TABLE 2: Recombination Rate Constants for the Organic Radicals Formed, at Different Oxygen Concentrations and pH Values

$2k/\epsilon$ (cm s^{-1})[a]	phenoxyl radical of gallic acid ($\lambda = 310$ nm)	Phenoxyl radical of gallate ion ($\lambda = 320$ nm)
argon saturation	$(2.0 \pm 1.0) \times 10^{6\,b}$	$(1.5 \pm 1.0) \times 10^{6\,b}$
air saturation	$(3.2 \pm 1.2) \times 10^{6\,b}$	$(1.0 \pm 0.4) \times 10^{6\,b}$
	$(3.09 \pm 0.01) \times 10^{6\,c}$	$(2.45 \pm 0.02) \times 10^{6\,c}$
oxygen saturation	$(2.6 \pm 1.0) \times 10^{6\,b}$	$(9.4 \pm 1.2) \times 10^{5\,b}$

[a] For each experimental condition at least four values of $2k/\epsilon$ are obtained from the fitting of the traces of independent experiments to the second-order law. The error bars stand for the standard deviations of these values. [b] Data obtained in CFP experiments with 1×10^{-2} M Na$_2$S$_2$O$_8$ solutions containing 5 μM gallic acid ($I = 0.03$ M). [c] Values obtained in LFP experiments with 5×10^{-2} M Na$_2$S$_2$O$_8$ solutions containing 10 μM gallic acid ($I = 0.15$ M).

for the reaction with gallic acid/gallate ion (see Table 1 for the rate constants) indicate that for LFP experiments in the presence of 50 μM of these substrates and otherwise identical conditions (see typical traces in the inset of Figure 3) at a time ca. 50 μs after the laser shot the contribution of the sulfate radical ions to the absorbance profiles should be negligible. Thus, the absorption spectra taken 50 μs after the shot are assigned to the organic radicals formed by reaction 2. Figures 2 and 3 show the absorption spectra taken 50 μs after the laser shot as well as at shorter times where the contribution of the sulfate radical to the traces cannot be neglected, at pH 3.1 and 5.4, respectively.

Under the CFP experimental conditions, depletion of SO$_4^{\bullet-}$ radicals takes place within less than 300 μs and thus at longer times after the flash of light absorption of both the organic radicals formed through reaction 2 and of their decay products is observed. The decay of the traces follows second-order kinetics (see below).

Since the interpretation of the CFP traces is complex, a bilinear regression analysis[36] was applied to the experimental matrix to obtain information on the absorption spectra of the species involved. The program shows that the absorbance at all the wavelengths can be expressed as a linear combination of the absorbance of two species. Taking the absorption spectra obtained in the LFP experiments for the organic radical, the spectra of the second species can be obtained. The decay of the shorter lived species (organic radical) and formation of the products obtained from the analysis of the traces at pH = 3.1 are shown in the inset of Figure 2. Since formation of the organic radical is too fast to be detected with our CFP setup, the spectra of the second species are due to the difference between the absorption of the products and that of the reactants. From the initial sulfate radical concentration (3.9×10^{-6} M) obtained from experiments without added gallic acid and otherwise identical conditions and assuming a total conversion of SO$_4^{\bullet-}$ to the organic radical, the absorption spectra of the products can be obtained (see Figures 2 and 3 for the data obtained at pH = 3.1 and 5.4, respectively).

Dwibedy et al.[37] investigated the reaction of HO$^\bullet$/O$^{\bullet-}$, N$_3^\bullet$, and Br$_2^{\bullet-}$ radicals with gallic acid at different pH values. They found that the corresponding phenoxyl radicals formed as transient species show a λ^{max} at 310 nm with a shoulder in the 400 nm region at pH 6.8, while those involved at pH $\geq$ 9.7 show λ^{max} at around 340 nm also with shoulders in the 400 nm region. The absorption spectrum of the phenoxyl radical[38] of methyl gallate shows a maximum at 310 nm at pH 3 with a broad shoulder in the 340−400 nm region, while that obtained at pH 7 has peaks at 340 and 420 nm and at 440 nm at pH 10.

Due to their similar shape and absorption coefficient values (see below), the spectra of the organic radicals obtained in the LFP experiments[39] are assigned to the phenoxyl radical of gallic acid (pH = 3.1) and gallate ion (pH = 5.4). Table 2 shows the
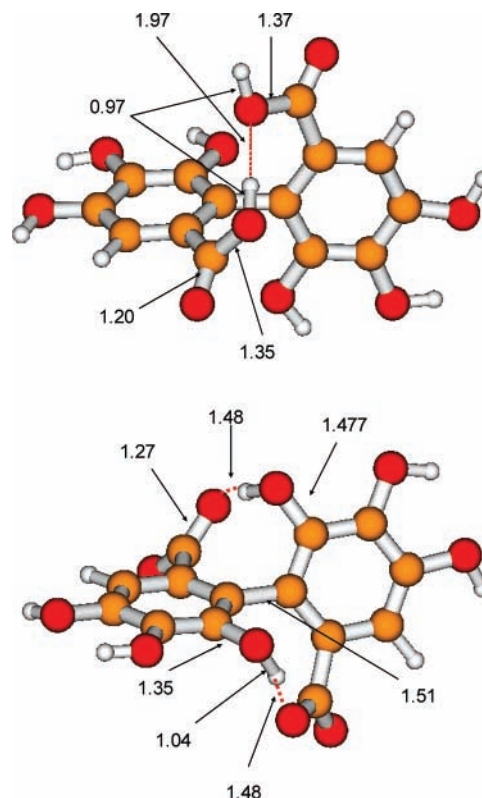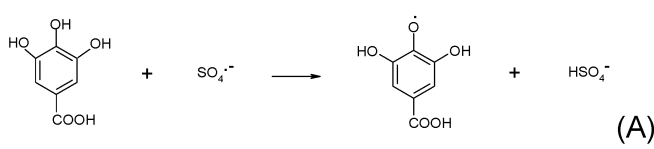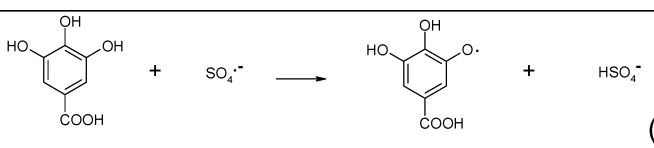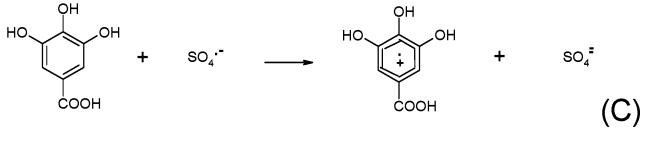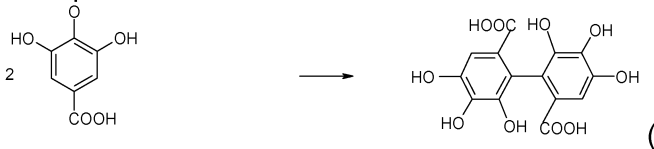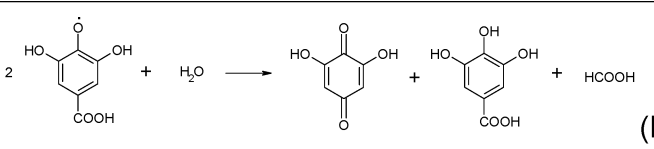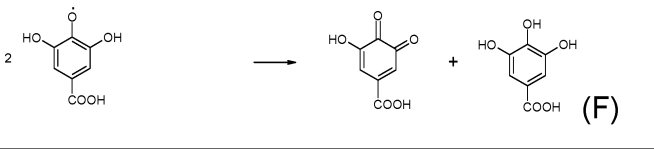

Figure 4. B3LYP/6-311++G**-optimized geometries of the biphenyls obtained in reactions (E) and (L), respectively. Distances are in Å.

values of $2k/\epsilon$ at the absorption maxima for the second-order recombination of the phenoxyl radicals obtained from reaction 2 at pH 3.1 and 5.4 under different oxygen concentrations. The oxygen independence of the values shown in Table 2 further supports the assignment to the phenoxyl radical.

The values of $2k/\epsilon$ obtained in LFP experiments performed with 5×10^{-2} M solutions of Na$_2$S$_2$O$_8$ at pH 5.4 (ionic strength, $I = 0.15$ M) are higher than those obtained with 1×10^{-2} M solutions of Na$_2$S$_2$O$_8$ ($I = 0.03$ M) in the CFP experiments, in line with the expected ionic strength effect on the rate constant for the recombination of two negatively charged species. However, the values of $2k/\epsilon$ obtained at pH 3.1 are independent of the ionic strength, as expected for the recombination of two uncharged species.

From the LFP experiments in the presence and absence of the substrate at both pH values the absorption coefficients of the phenoxyl of gallic acid at 310 nm and gallate ion at 320 nm are found to be 8.1×10^3 and 4.8×10^3 M^{-1} cm^{-1}, respectively. These values yield $2k = 2.5 \times 10^{10}$ M^{-1} s^{-1} at pH 3.1. The ionic strength-dependent rate constant $2k$ (pH = 5.4) is 4.8×10^9 M^{-1} s^{-1} at $I = 0.03$ M and 1.2×10^{10} M^{-1} s^{-1} at $I = 0.15$ M. Recombination rate constants close to

TABLE 3: Calculated ΔE° Values for the Reactions Involving Gallic Acid or Its Phenoxyl Radical in the Gas and in Aqueous Phase and ΔH° and ΔG° for the Gas-Phase Reactions at 298.15 K (all quantities are in kcal/mol)

Reactions	ΔE^0	ΔE^0 (aq)	ΔH^0	ΔG^0
(A)	-18.50	-27.21	-12.62	-18.72
(B)	-17.87	-23.16	-17.94	-18.11
(C)	223.76	137.88	223.39	223.83
(D)	-27.57	-24.28	-27.09	-13.19
(E)	-2.94	-4.05	-3.40	-4.27
(F)	-3.31	-4.73	-2.66	-3.31

diffusion-controlled values were also reported for unsubstituted phenoxyl radicals.[40]

Theoretical Calculations. To further support formation of the phenoxyl radicals of the different species of gallic acid and investigate the mechanism of formation of these species, DFT calculations were performed.

Formation of the phenoxyl radicals as first products of reaction 2 can take place through the following different pathways.

(a) Electron transfer from gallic acid to the sulfate radical anion leading to formation of the radical cation of gallic acid and the sulfate anion. The radical cation undergoes a fast reversible hydration to yield hydroxycyclohexadienyl (HCHD) radicals.[40] Water elimination from HCHD radicals of phenols, yielding phenoxyl radicals has been reported.[39,41]

(b) The addition/elimination route leading to a sulfate radical adduct followed by elimination of sulfate anion or sulfite anion yielding HCHD or phenoxyl radicals, respectively.[42]

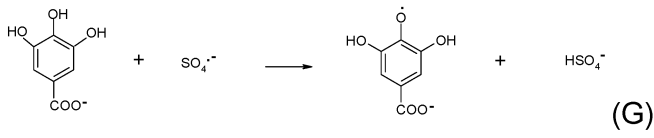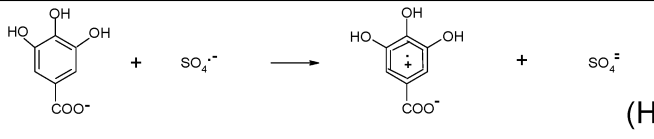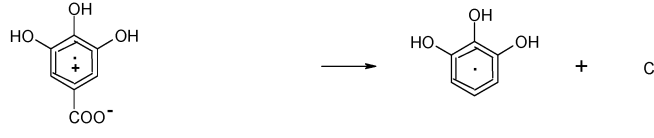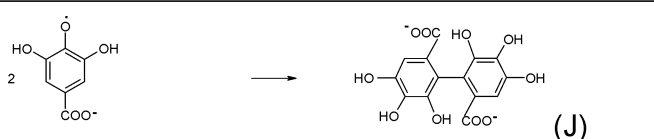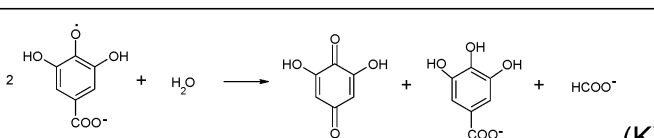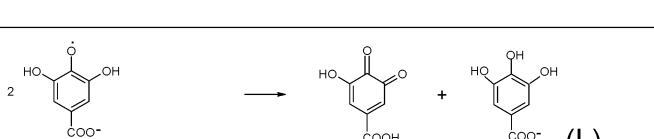(c) H abstraction from the phenol to the sulfate radical anion.[43]

The theoretical results are summarized in Tables 3 and 4. Calculations obtained for reactions A and B in Table 3 and G

in Table 4 show that the H-abstraction processes from the O—H groups are exothermic and thermodynamically feasible. One-electron charge-transfer processes from gallic acid or gallate ion to the sulfate radical leading to formation of the corresponding radical cations (processes C and H) are endothermic as well as proton elimination necessary to form the phenoxyl radicals from the radical cations (processes not shown in the tables). On the other hand, all attempts to obtain a direct addition of the sulfate radical to the ring were unsuccessful, as the approach to the phenolic groups of the gallic acid or gallate ion is highly favored, indicating the addition/elimination route is not feasible.

In summary, the results show that the reaction takes place through the H-abstraction route. This is also the case for other benzene derivatives with two OH substituents in the ortho position.[43]

On the basis of the observation of a second-order recombination of the phenoxyl radicals both at pH 3.1 and 5.4 (see Table 2), the ΔE°, ΔH°, and ΔG° values for the different recombination reaction pathways[44] were calculated. Both formation of biphenyls (reactions D) and disproportionation to yield quinones

TABLE 4: Calculated $\Delta E°$ Values for the Reactions Involving the Gallate Anion or Its Phenoxyl Radical in the Gas and Aqueous Phase and $\Delta H°$ and $\Delta G°$ for the Gas-Phase Reactions at 298.15 K (all quantities are in kcal/mol)

Reactions	ΔE^0	ΔE^0 (aq)	ΔH^0	ΔG^0
(G)	-29.10	-30.88	-29.33	-29.32
(H)	115.70	141.60	115.43	115.65
(I)	0.17	82.43	0.71	-9.79
(J)	26.01	(a)	25.63	41.87
(K)	16.77	5.72	16.29	15.92
(L)	0.98	-4.30	1.64	5.02

[a] Not included due to technical problems.

from the protonated phenoxyl radicals (reactions E and F) resulted in exothermic and thermodynamically feasible pathways. The optimized structures along with the most relevant geometrical parameters of biphenyls are reported in Figure 4. For the carboxylate anion of the phenoxyl radical disproportionation reaction L is more favorable than reactions J and K.

The weight of a recombination at the oxygen atom to yield an organic peroxide is assumed to be nonsignificant because of the low O−O binding energy of the resulting product,[44] which would tend to make this reaction reversible. In fact, all theoretical calculations performed on reaction products containing O−O bonds were unsuccessful as the system readily breaks the O−O bond during the geometry optimization process. Mixed carbon−oxygen coupling has also been reported,[45] although these reactions were not considered.

Product Analysis. To confirm the theoretical predictions about the products of reaction 2, the irradiated solutions were analyzed by the NBT test and HPLC/MS. The response to the NBT quinones test was positive for solutions of pH 3.1 and 5.4. The HPLC/MS analysis of solutions of pH 5.4 shows

formation of the quinone (product of reaction L in Table 4). This reaction is expected to be the most favorable pathway (see above).

Conclusions

Flash photolysis, DFT calculations, and chromatographic product analysis confirm the proposed reaction mechanism, which includes the involvement of the phenoxyl radicals as intermediates of the sulfate radical-mediated oxidation of gallic acid and gallate anion. The calculations support the phenoxyl radicals recombination to yield substituted biphenyls and quinones.

Extrapolation of the chemistry of the phenoxyl radicals of gallic acid to that of the humic phenoxyl radicals is not straightforward. For instance, the chance of humic phenoxyl radicals to yield recombination products is very likely affected by the presence of metal ions, which efficiently complex these radicals,[46] and by the environmental microheterogeneity of natural waters, where humic substances aggregate.[47]

Caregnato et al.

References and Notes

(1) Nakayasu, K.; Fukushima, M.; Sasaki, K.; Tanaka, S.; Nakamura, H. *Environ. Toxicol. Chem.* **1999**, *18*, 1085−1090.

(2) Schnitzer, M.; Khan, S. U. *Humic Substances in The Environments*; Marcel Dekker: New York, 1972; p 203.

(3) Chiou, C. T.; Malcolm, R. L.; Briton, T. I.; Kile, P. E. *Environ. Sci. Technol.* **1986**, *20*, 502−508.

(4) Saiz-Jimenez, C. *Environ. Sci. Technol.* **1994**, *28*, 1773−1780.

(5) Waite, T. D.; Morel, F. M. M. *J. Colloid Interface Sci.* **1984**, *102*, 121−137.

(6) Scott, D. T.; McKnight, D. M.; Blunt-Harris, E. L.; Kolesar, S. E.; Lovley, D. R. *Environ. Sci. Technol.* **1998**, *32*, 2984−2989.

(7) Lovley, D.; Coates, J.; Blunt-Harris, E.; Phillips, E.; Woodward, J. *Nature* **1996**, *382*, 445−448.

(8) Coates, J.; Ellis, D.; Blunt-Harris, E.; Gaw, C.; Roden, E.; Lovley, D. *Appl. Environ. Microbiol.* **1998**, *64*, 1504−1509.

(9) Struyk, Z.; Sposito, G. *Geoderma* **2001**, *102*, 329−346.

(10) Thorn, K.; Arterburn, J.; Mikita, M. *Environ. Sci. Technol.* **1992**, *26*, 107−116.

(11) Senesi, N. *Adv. Soil Sci.* **1990**, *14*, 77−130.

(12) Senesi, N.; Loffredo, E. In *Soil Physical Chemistry*; Sparks D. L., Ed.; CRC Press: Boca Raton, FL, 1999; pp 239−370.

(13) Liang, C.; Bruell, C. J.; Marley, M. C.; Sperry, K. L. *Chemosphere* **2004**, *55*, 1225−1233.

(14) Gates, D. D.; Siegrist, R. L. *J. Environ. Eng.* **1995**, *121*, 639−644.

(15) Amarante, D. *Pollut. Eng.* **2000**, 32, 40−42.

(16) MacKinnon, L. K.; Thomson, N. R. *J. Contam. Hydrol.* **2002**, *56*, 49−74.

(17) House, D. A. *Chem. Rev.* **1962**, 62, 185−203.

(18) Anipsitakis, G. P.; Dionysiou, D. D. *Environ. Sci. Technol.* **2003**, *37*, 4790−4797.

(19) Tipping, E. *Cation Binding by Humic Substances*, 1st ed.; Cambridge University Press, Cambridge, U.K., 2002.

(20) Stevenson, F. J. *Humus Chemsitry. Genesis*, *Composition*, *Reactions*, 2nd ed.; John Wiley and Sons: New York, 1994.

(21) Giannakopoulos, E.; Christoforidis, K. C.; Tsipis, A.; Jerzykiewicz, M.; Deligiannakis, Y. *J. Phys. Chem. A.* **2005**, *109*, 2223−2232.

(22) Zheng, W. S.; Wang, Y. *J. Agric. Food. Chem.* **2001**, *49*, 5165−5160.

(23) Alegre, M. L.; Geronés, M.; Rosso, J. A.; Bertolotti, S. G.; Braun, A. M.; Mártire, D. O.; Gonzalez, M. C. *J. Phys. Chem. A.* **2000**, *104*, 3117−3125.

(24) Dwibedy, P.; Dey, G. R.; Naik, D. B.; Kishore, K.; Moorthy, P. N. *Phys. Chem. Chem. Phys.* **1999**, *1*, 1915−1918.

(25) Paz, M. A.; Flückiger, R.; Boak, A.; Kagan, H. M.; Gallop, P. M. *J. Biol. Chem.* **1991**, *266*, 689−692.

(26) Becke, A. D. *J. Chem. Phys.* **1993**, *98*, 5648−5652.

(27) Lee, C.; Yang, W.; Parr, R. G. *Phys. Rev. B.* **1988**, *37*, 785−789.

(28) Krishnan, R.; Binkley, J. S.; Seeger, R.; Pople, J. A. *J. Chem. Phys.* **1980**, *72*, 650−654.

(29) Clark, T.; Chandrasekhar, J.; Spitznagel, G. W.; Schleyer, P. V. R. *J. Comput. Chem.* **1983**, *4*, 294−301.

(30) Frisch, M. J.; Pople, J. A.; Binkley, J. S. *Chem. Phys.* **1984**, *80*, 3265−3269.

(31) Frisch, M. J.; Trucks, G. W.; Schlegel, H. B.; Scuseria, G. E.; Robb, M. A.; Cheeseman, J. R.; Montgomery, J. A., Jr.; Vreven, T.; Kudin, K. N.; Burant, J. C.; Millam, J. M.; Iyengar, S. S.; Tomasi, J.; Barone, V.; Mennucci, B.; Cossi, M.; Scalmani, G.; Rega, N.; Petersson, G. A.; Nakatsuji, H.; Hada, M.; Ehara, M.; Toyota, K.; Fukuda, R.; Hasegawa, J.; Ishida, M.; Nakajima, T.; Honda, Y.; Kitao, O.; Nakai, H.; Klene, M.; Li, X.; Knox, J. E.; Hratchian, H. P.; Cross, J. B.; Bakken, V.; Adamo, C.; Jaramillo, J.; Gomperts, R.; Stratmann, R.E.; Yazyev, O.; Austin, A. J.; Cammi, R.; Pomelli, C.; Ochterski, J. W.; Ayala, P.Y.; Morokuma, K.; Voth, G. A.; Salvador, P.; Dannenberg, J. J.; Zakrzewski, V. G.; Dapprich, S.; Daniels, A. D.; Strain, M.C.; Farkas, O.; Malick, D. K.; Rabuck, A. D.; Raghavachari, K.; Foresman, J. B.; Ortiz, J. V.; Cui, Q.; Baboul, A. G.; Clifford, S.; Cioslowski, J.; Stefanov, B. B.; Liu, G.; Liashenko, A.; Piskorz, P.; Komaromi, I.; Martin, R.L.; Fox, D. J.; Keith, T.; Al-Laham, M. A.; Peng, C. Y.; Nanayakkara, A.; Challacombe, M.; Gill, P. M. W.; Johnson, B.; Chen, W.; Wong, M. W.; Gonzalez, C.; Pople, J. A. *Gaussian 03*, Revision C.02; Gaussian, Inc.: Wallingford, CT, 2004.

(32) Miertos, S.; Tomasi, J. *Chem. Phys.* **1982**, *65*, 239−245.

(33) Cossi, M.; Barone, V.; Cammi, R.; Tomasi, J. *Chem. Phys. Lett.* **1996**, *255*, 327−355.

(34) Barone, V.; Cossi, M.; Menucci, B.; Tomasi, J. *J. Chem. Phys.* **1997**, *107*, 3210−3221.

(35) McElroy, W. J.; Waygood, S. J. *J. Chem. Soc., Faraday Trans.* **1990**, *86*, 2557−2564.

(36) San Román, E. A.; Gonzalez, M. C. *J. Phys. Chem.* **1989**, *93*, 3532−3536.

(37) Dwibedy, P.; Dey, G. R.; Naik, D. B.; Kishore, K.; Moorthy, P. N. *Phys. Chem. Chem. Phys.* **1999**, *1*, 1915−1918.

(38) Jovanovic, S. V.; Hara, Y.; Steenken, S.; Simic, M. G. *J. Am. Chem. Soc.* **1995**, *117*, 9881−9888.

(39) Draper, P. B.; Fox, M. A.; Pelizetti, E.; Serpone, N. *J. Phys. Chem.* **1989**, *93*, 1938−1943.

(40) Merga, G.; Aravindakumar, C. T.; Rao, B. S. M.; Mohan, H.; Mittal, J. P. *J. Chem. Soc.*, *Faraday Trans.* **1994**, *90*, 597−604.

(41) Adams, G. E.; Mitchel, B. D.; Land, E. J. *Nature* **1966**, *211*, 293−294.

(42) Mártire, D. O.; Gonzalez, M. C. *Prog. React. Kinet. Mech.* **2001**, *26*, 201−218.

(43) Leopoldini, M.; Marino, T.; Russo, N.; Toscano, M. *J. Phys. Chem. A.* **2004**, *108*, 4916−4922.

(44) Fang, X.; Schuchmann, H. P.; von Sonntag, C. *J. Chem. Soc., Perkin Trans. 2* **2000**, 1391−1398.

(45) Hunter, W. H.; Morse, M. *J. Am. Chem. Soc.* **1926**, *48*, 1615.

(46) Rotthaus, O.; Jarjayes, O.; Thomas, F.; Philouze, C.; Saint-Aman, E.; Pierre, J.-L. *Dalton Trans.* **2007**, 889−895.

(47) Latch, D. E.; McNeill, K. *Science* **2006**, *311*, 1743−1747.